Biomimetic Formation of Hydroxyapatite Nanorods by a Single-Crystal-to-Single-Crystal Transformation

ARTICLE *in* ADVANCED FUNCTIONAL MATERIALS · DECEMBER 2005

Impact Factor: 11.81 · DOI: 10.1002/adfm.200500274

4 AUTHORS, INCLUDING:

Jinhua Zhan
Shandong University
128 PUBLICATIONS **3,650** CITATIONS
SEE PROFILE

Jerry Chan
National Taiwan University
95 PUBLICATIONS **2,385** CITATIONS
SEE PROFILE

Chung-Yuan Mou
National Taiwan University
380 PUBLICATIONS **13,422** CITATIONS
SEE PROFILE

ADVANCED FUNCTIONAL MATERIALS

Biomimetic Formation of Hydroxyapatite Nanorods by a Single-Crystal-to-Single-Crystal Transformation**

By *Jinhua Zhan*, *Yao-Hung Tseng*, *Jerry C. C. Chan*, and *Chung-Yuan Mou**

Uniform nanorods of hydroxyapatite (HAP) with an unusual orthorhombic shape have been synthesized from homogeneous solutions of Ca^{2+} and HPO_4^{2-} in the presence of gelatin and urea. The lengths of the nanorods are in the range of hundreds of micrometers, and the widths are about 100 nm. The HAP phase is generated by the transformation from its precursor phase of octacalcium phosphate (OCP), which has been monitored by X-ray diffraction, NMR spectroscopy, scanning electron microscopy, and transmission electron microscopy. The rise in pH due to the decomposition of urea drives the OCP transformation to HAP. In the presence of gelatin, nanorods of OCP phase formed first and then transformed into the HAP phase, preserving the single-crystal morphology. On the other hand, blade-like OCP crystals form from the solution in the absence of gelatin. On increasing the pH of the solution, the large, blade-like OCP crystals tend to crash into irregular, hexagonal HAP crystallites. A single-crystal-to-single-crystal topochemical transformation may be attributed to the evolution of HAP nanorods from the precursor OCP phase. This gives a strong indication as to the OCP to HAP transformation mechanism in the mineralization of biological apatite in tooth enamel and bone.

1. Introduction

Single-crystal-to-single-crystal transformation as a mode of solid-state reaction has received a lot of recent attention for its preservation of crystal morphology.[1] Most of these types of reaction involve only minimum movements of the molecules in topochemical reactions, such as in geometrical isomerization,[2] polymerizations on prearranged monomers,[3] loss of hydration water,[4] or guests in host–guest molecular solids.[5] Large movements of molecules inside a single crystal would most likely lead to crystal disintegration. When the size of the crystals decreases to the nanometer size range, however, the preservation of crystal morphology would become increasingly possible. This would be highly advantageous in biomimetic fabrication of materials where hierarchical organization of inorganic/organic materials is desired.[6] When inorganic nanocrystals within a hierarchical organization undergo physicochemical transformation, the higher-order organizations may still be preserved.

Biomineralization often involves nanocrystals in the lowest level of hierarchical organization. An important example is hydroxyapatite (HAP), nanocrystals of which are embedded among biomolecules in bones and teeth.[7] The main inorganic component of bone and teeth is made from calcium phosphate in the form of the mineral HAP associated with a large number of biomolecules.[8] HAP ($Ca_{10}(PO_4)_6(OH)_2$) is the most stable and least soluble in water among the calcium phosphates. There is increasing evidence that it is transformed in vivo from precursor crystals, such as octacalcium phosphate (OCP, $Ca_8(HPO_4)_2(PO_4)_4{\cdot}5H_2O$). The presence of HPO_4^{2-} groups in bone apatites suggests OCP is a precursor. This hypothesis is further supported by the presence of an OCP "central dark line" in HAP in tooth enamel.[9] Herein, we report on the transformation from OCP to HAP[10] and its impact on the crystal morphology in a gelatin matrix. We report the preparation of HAP nanorods with a high aspect ratio which form through a shape-preserving single-crystal-to-single-crystal transformation from OCP nanorods.

The most common form of HAP is hexagonal and the crystal structure is generally described to the space group $P6_3/m$ (176) with lattice parameters $a = b = 9.432$ Å, $c = 6.881$ Å and $Z = 1$.[11] Hexagonally shaped apatite particles can usually be synthesized by solution-based or high-temperature techniques, which obey the hexagonal crystallographic nature of HAP.[12] Bones are composed of mineralized collagen fibrils, which are composites of nanometer-sized biological apatite within the collagen and gelatin matrix. The inorganic HAP nanocrystals in bone are platelet shaped and elongated along the crystallographic *c*-axis.[11,13]

The transformation of OCP to HAP may be initiated by raising the pH from acidic to alkaline. Hydroxyapatite only forms when the pH is higher than 7.4.[14] However, one needs a method of raising the pH of the solution uniformly to avoid inhomogeneity in solution mixing. Previously, we have used the decomposition of urea for fabricating a unique form of porous single-crystalline calcium carbonate in the presence of gelatin.[15] Here, we employ a similar method of urea decomposition to ensure the uniformity of pH for the study of the OCP to HAP transformation.

It is well known that biomolecules may strongly influence crystal polymorphism and the morphology of biogenic inorgan-

[*] Prof. C.-Y. Mou, Dr. J. Zhan, Y.-H. Tseng, Prof. J. C. C. Chan
Department of Chemistry and Center of Condensed Matter
National Taiwan University
Taipei, 106 (Taiwan)
E-mail: cymou@ntu.edu.tw

[**] This work was supported by a grant from the MOE Program for Promoting Academic Excellence of Universities.

 DOI: 10.1002/adfm.200500274

ic crystals by preferential surface adsorption. For our purposes, we first chose a biomolecule that would help the formation of nanocrystals of OCP. We could then study the OCP to HAP transformation. In the literature, the gelatin matrix has also been used to study biomineralization under various conditions.[16–18] Also, in our previous use of gelatin in generating nanocrystals of vaterites (one of the polymorphs of $CaCO_3$),[15] it was shown that gelatin interacts strongly with calcium ions to protect the nanocrystal. Recently, it has been reported that polypeptides with negatively charged carboxylate groups, such as polyaspartates or bovine amelogenin, can also strongly modify the structure and morphology of OCP.[19–21]

2. Results and Discussion

First, we examined a large area of the final product obtained after a 96 h reaction by scanning electron microscopy (SEM). One can see from Figure 1 that the product consists of bundles of nanorods. The lengths are in the range of hundreds of micrometers, and the nanorods are about 100 nm wide. The morphology of the products was further examined by SEM (Figs. 2A,B) and transmission electron microscopy (TEM; Fig. 3) under higher magnification. Figure 2A shows the ends of these nanorods; the inset shows a rectangular cross-section. Figure 2B shows a lateral view of a *single* nanorod. This orthorhombic shape is rather unusual, since HAP crystals prepared in vitro are mostly in the form of hexagonal rods.[12] Figure 3A depicts a typical TEM image of the HAP nanorods. The spots on the corresponding selected-area electron diffraction (SAED) pattern, shown in the upper part of Figure 3B, can be indexed to the [210] zone axis of a hexagonal HAP crystal, in accordance with the simulated electron diffraction pattern of HAP crystals along the [210] zone axis (Fig. 3C). Streaking of the reflections in the underfocused electron diffraction pattern, shown in the lower part of Figure 3B, implies that the preferred growth direction of the HAP nanorods is along the [001] orientation. Normally, the (001) reflection is kinematically forbidden for HAP because it has a structure factor $F=0$. Weak (001) reflections can be present in the electron diffraction pattern owing to dynamic scattering events, although they are kinematically forbidden.[22]

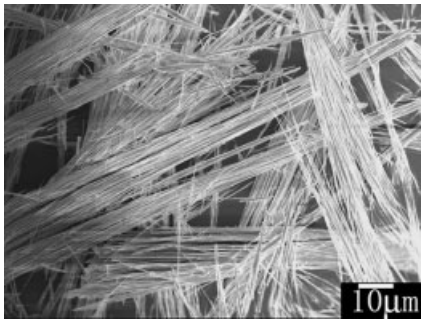

Figure 1. Overview SEM image of HAP obtained after 96 h in the presence of gelatin.

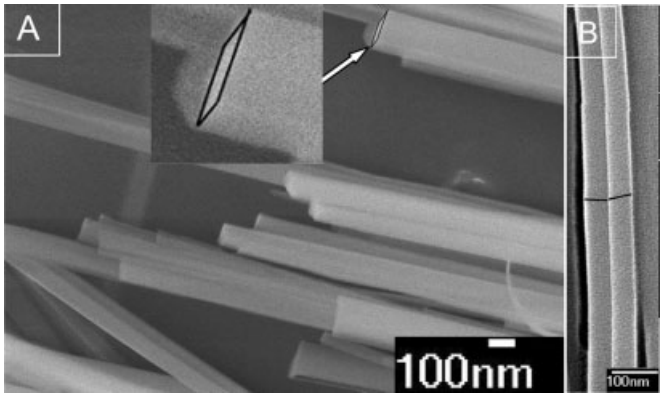

Figure 2. A) SEM image of HAP nanorods. Inset: typical orthogonal shape. B) Lateral view of a HAP nanorod.

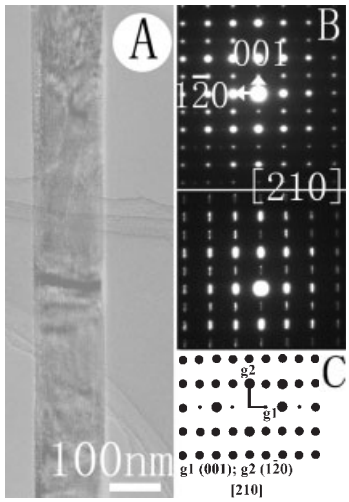

Figure 3. A) TEM image of a single HAP nanorod. B) Selected-area electron diffraction (SAED) pattern (upper part) and an underfocused SAED pattern (lower part). C) Simulated electron diffraction pattern along the [210] zone axis of the HAP crystal.

In the X-ray diffraction (XRD) measurements, HAP nanorods generally lay on the sample cell. XRD measurements show that all diffraction peaks of the as-obtained sample can be assigned to hexagonal HAP (Joint Committee for Powder Diffraction Standards, JCPDS, 01-086-0740), as shown in Figure 4 (obtained at 96 h). The XRD pattern appears to be much simplified compared to that of the usual three-dimensional (3D) HAP crystals. The relative intensity of the (*hk*0) diffraction peaks is unusually strong, and the (00*l*) diffraction peaks are missing in the XRD patterns. This also suggests a highly preferred orientation of the HAP nanorods along the [001] direction. XRD patterns from samples collected after various reaction times are shown in Figure 4. The product collected after 2 h can be identified as phase-pure OCP ($Ca_8(HPO_4)_2(PO_4)_4{\cdot}5H_2O$), as indicated by the triangles in Figure 4. One observes an OCP to HAP transformation, and the Ca/P ratios increase gradually from 1.33 at 2 h to 1.42 at 6 h, and finally to 1.64 at 96 h.

ADVANCED FUNCTIONAL MATERIALS

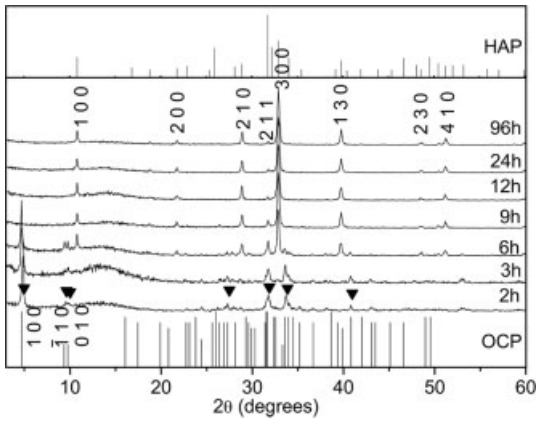

Figure 4. XRD pattern of products obtained after various reaction times. Top: standard pattern of HAP from JCPDS 01-086-0740; bottom: standard pattern of OCP from JCPDS 44-0778.

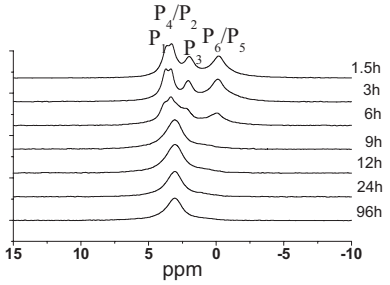

Figure 6. ^{31}P MAS NMR spectra of products obtained in the presence of gelatin after various reaction times.

The morphology of OCP is also rod-like, with the same dimensions as HAP, as shown in Figure 5A. In fact, before and after the transformation from OCP to HAP, the products at various times always appeared rod-like with equal sizes. The morphology of products obtained in the presence of gelatin at various reaction times is demonstrated in Figures 5A–D. The change of crystal structure from OCP to HAP seems to be accomplished with the preservation of the shape and size of the rod-shaped crystal. There was no observable fragmentation of the crystals.

Furthermore, the ^{31}P magic-angle spinning (MAS) NMR spectrum (Fig. 6) of the 3 h sample (OCP) reveals four peaks at 0.2, 2.0, 3.3, and 3.7 ppm, corresponding to the P5/P6, P3, P2/P4, and P1 crystallographic sites, respectively (see Fig. 7B).[23] As the reaction time increased, the four peaks became broader, finally transforming to a single peak around 3 ppm, assigned to HAP. It is notable that the 6 h spectrum is not a superposition of the 3 h (OCP) and 9 h (HAP) spectra. Therefore, it is unlikely that HAP forms by re-precipitation, and we believe this is a result of OCP to HAP transformation.

In the absence of gelatin in the reaction solution, XRD measurements indicate that OCP was also obtained at the initial stages of reaction, and HAP was obtained at longer reaction times (Fig. 8). Figure 8 shows the XRD pattern of the transition from OCP to HAP. It appears quite similar to the transformation in the presence of gelatin, except that it takes a little longer for OCP to transform into HAP, which may be due to the much thicker crystals of OCP. The initial crystal morphology of OCP obtained in the absence of gelatin is blade-like with wide (100) faces, several micrometers wide and elongated along the *c*-axis (Fig. 9A). The crystal shown in Figure 9A is bordered by the characteristic (011) and (010) faces. After transformation to HAP, the large, blade-like OCP crystal splits along the *c*-axis into many hexagonal rod-shaped crystallites owing to the loss of water, so that many slits between crystallites were left (Fig. 9B).[10c] We further see that a blade-like crystal is divided into two layers. One layer is made up of many hexagonal crystallites. The inset clearly shows the hexagonal shape of the rod tip, and Figure 9C gives a schematic diagram of a hexagonal HAP rod. A SEM image (Fig. 10) of a large area of the product obtained after 96 h treatment in the absence of gelatin shows extensive fragmentation of the original blade-like crystal. Apparently, without the protection of gelatin, the starting OCP crystals are too thick to withstand the stress of the transformation to the HAP structure.

In order to understand the transformation of the OCP to the HAP structure, we first examined their crystal structures. The crystallographic relationship between HAP and OCP was previously examined by Brown et al.[13] The unit cell of OCP is triclinic, space group *P*1, which can be described in terms of alternating apatite and hydrated layers parallel to the (100) plane. The

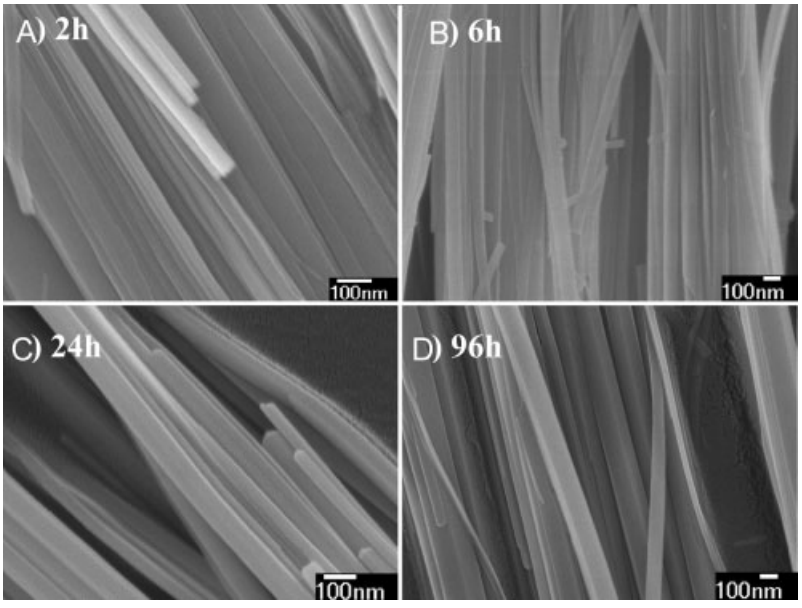

Figure 5. SEM images of the products obtained in the presence of gelatin at various reaction times: A) 2 h, B) 6 h, C) 24 h, and D) 96 h. One can see the same nanorod morphology for both OCP and HAP.

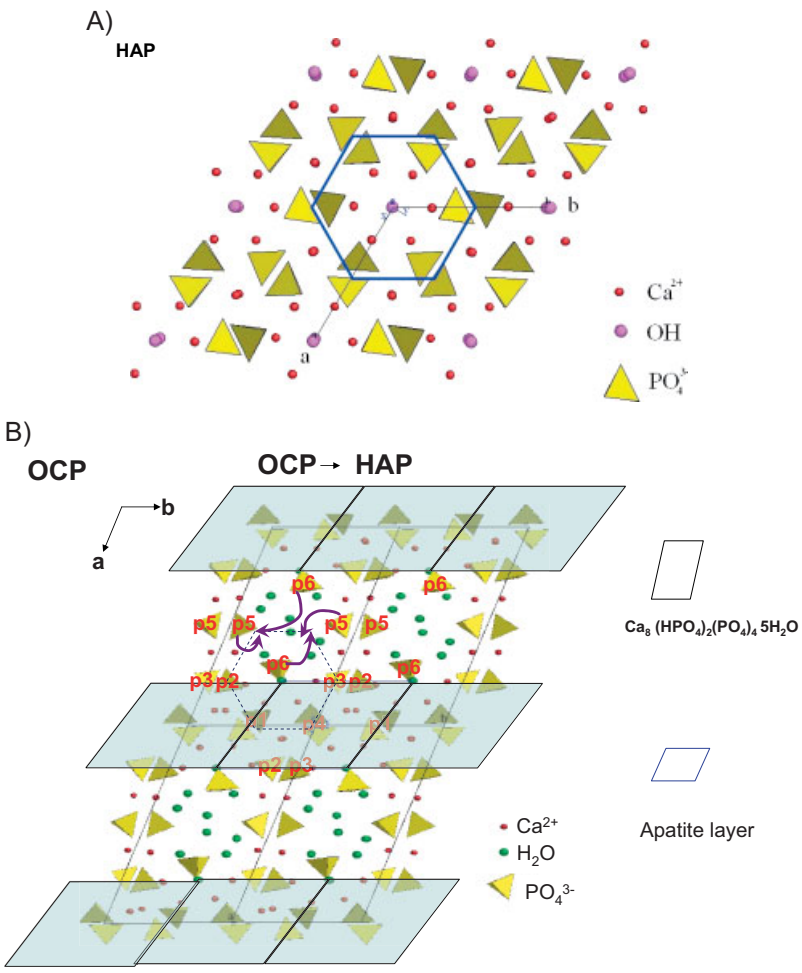

Figure 7. Crystal structure of A) HAP and B) OCP. The central parallelogram (B) indicates the apatite unit, and the six crystallographic sites in OCP are labeled. Possible movement of P5 and P6 in an OCP crystal to generate a HAP structure is demonstrated.

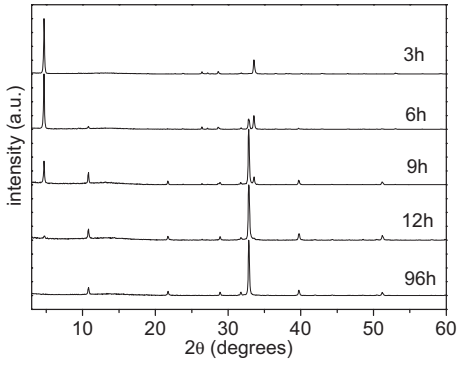

Figure 8. XRD patterns of the evolution from OCP to HAP phases at various reaction times in the absence of gelatin.

unique similarity of OCP to the structure of HAP (see Figs. 7A,B) and its thermodynamic metastability attracts attention for its possible role as a precursor during the mineralizing process of biological apatites.[9] The experimental results indicate that gelatin molecules have a considerable effect on the morphology of OCP, and finally on HAP. The gelatin used in our experiments was derived from lime-cured bovine skin. It is proteinaceous in nature, and dominated by carboxylate amino acids, such as glutamate and aspartate.[24] Recently, it has been shown by Bigi et al.[19] that polyglutamate and polyaspartate can inhibit the OCP to HAP transformation owing to their strong adsorption on the surfaces of OCP. There are specific interactions between polyaspartate and the OCP structure which allow the control of morphology.[19] Iijima et. al.[20,21] reported that bovine amelogenins can suppress the growth of OCP in the *b*-axis direction. Hence, rod-like crystals are generated instead of the typical ribbon-like OCP crystals. Thus, we suggest that in the initial stages of reaction between Ca^{2+} with HPO_4^{2-}, OCP particles precipitate, with the lateral faces (*a* and *b* directions) adsorbed by the gelatin macromolecules. Addadi and co-workers[25] have found that the cell-adhesion protein fibronectin molecules preferentially adsorb to the ionic surface of calcite, while they desorb from the layers of lattice water of brushite. It seems that gelatin molecules also avoid binding to the surface perpendicular to the *c*-axis, where the lattice water molecules of OCP are exposed. On the other hand, it tightly adsorbs to the other, more ionic surfaces. This leads to a large growth anisotropy, and thus to the long, rod-like shape of the OCP crystallites under the protection of gelatin. OCP is only stable in an acidic environment.[8,14] Initially, the pH of the reaction solution was 4.58. With the increase in solution pH caused by the slow decomposition of urea, these OCP nanorods transformed into HAP nanorods. After the reaction had proceeded for 96 h, the pH of the solution had reached about 8.88.

Without the presence of gelatin, the loss of water in the OCP to HAP transformation would create a large stress in the crystal and lead to an irregular fragmentation of the crystal. On the other hand, under the protection of the gelatin molecules, the long, rod-shaped OCP crystallites apparently have small enough dimensions along the *a* and *b* directions to allow a single-crystal-to-single-crystal transformation. Structurally speaking, the "hydrated layer" in OCP crystals (Fig. 7B) is composed of hydrated channels along the *c*-axis, which allow the transport of ions to form new structures. The "hydrated layer" is partitioned along the *b*-axis by Ca^{2+} and HPO_4^{2-} that connect the neighboring apatite layers by strong bonds along the *a*-axis. As demonstrated by the NMR data (Fig. 6) and the crystallographic relationship between OCP and HAP (see Fig. 7), the HPO_4^{2-} ions (P5 and P6) in the hydrated layers of an OCP crystal have to move during the transition process from OCP to HAP. This movement is denoted by arrows in Figure 7B. Although there is only 2.1 % mismatch between the (100)

ADVANCED FUNCTIONAL MATERIALS

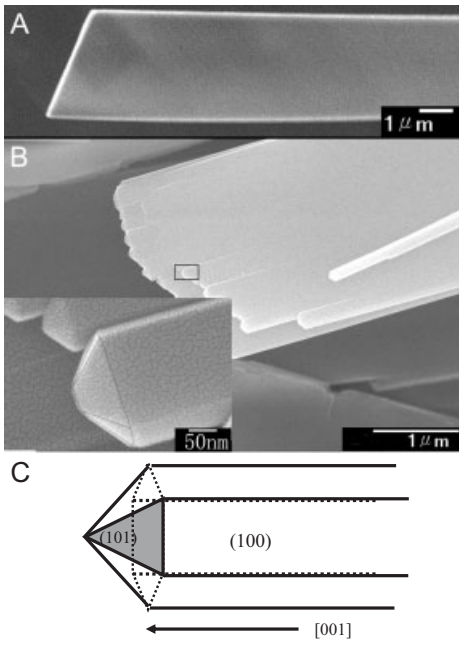

Figure 9. A) A typical blade-like OCP crystal. B) A broken unit composed of HAP crystallites; the inset is a magnified view of the selected area. C) Schematic diagram of HAP hexagonal crystallites.

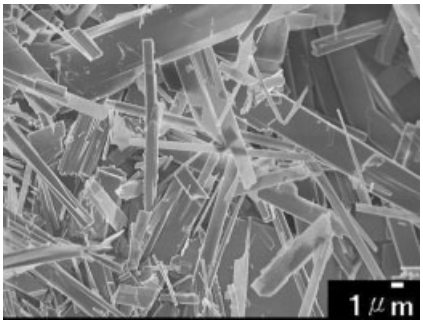

Figure 10. An overview SEM image of HAP crystals obtained after 96 h in the absence of gelatin.

crystal plane of OCP and the (100) crystal plane of HAP ($b_{OCP} = 9.630$ Å, JCPDS 44-0778, $b_{HAP} = 9.432$ Å, JCPDS 24-0033), the apatite layers in the large, blade-like OCP crystals have to split along the *b*-axis of OCP to form HAP. Moreover, the loss of water during the transition process from OCP to HAP may cause the shrinkage of apatite layers along a direction perpendicular to the (100) crystal planes, keeping in mind the interplanar spacing difference between $(100)_{OCP}$ and $(100)_{HAP}$ ($d_{100,OCP} = 18.60$ Å, $d_{100,HAP} = 8.168$ Å, $d_{100,OCP} - 2d_{100,HAP} = 2.264$ Å). The movement of P5 and P6, a small crystallographic mismatch, and the loss of water may cause a recrystallization of apatite layers in OCP, which can subsequently result in the generation of hexagonal HAP rods in an OCP crystal with only the *c*-axis preserved. Figure 9B shows two layers of HAP rods are generated in a large blade-like crystal. The slits between HAP rods are obvious, as demonstrated by the inset of Figure 9B.

The initial lateral width of OCP along the *a*- and *b*-axes had a considerable effect on the transformation to HAP. Initially, OCP nanorods were generated in the presence of gelatin. During the transition process from OCP to HAP, the apatite layers bound with gelatin molecules may act as substrates for the movement of HPO_4^{2-} and the loss of crystal-lattice water to form HAP. Both theoretical calculations and in-vitro studies have also shown that HAP is able to grow epitaxially on the (100) surface of OCP in such a way that the *c*-axes of HAP and OCP are parallel to each other.[26] The OCP nanorods along lateral dimensions can endure the impact of the small crystallographic mismatch and dehydration. This may be the reason that OCP transforms into HAP with the preservation of the orthorhombic nanorod morphology. However, when the lateral width of the (100) crystal planes in an OCP crystal becomes too large, the small mismatch may become too large to sustain a single-crystal-to-single-crystal transformation.

Single-crystal-to-single-crystal transformation into HAP may take place in the formation of biological apatites in bones or teeth.[27] It would be a highly advantageous mechanism, since the higher hierarchical structures would be preserved. In biological apatite, crystallites in the bone are about 50 nm × 25 nm × 4 nm, elongated along the *c*-axis. Our synthetic HAP nanorods have a much longer *c*-axis; nonetheless, we did produce orthorhombic crystals with elongation along the *c*-axis. The special shape of the long HAP nanorods with rectangular cross-section was obtained from the precursor OCP phase, with the preservation of the crystal morphology.

3. Conclusion

In summary, we have obtained HAP nanorods by homogeneous precipitation of OCP nanorods in the presence of gelatin. The experimental results and crystallographic analyses reveal that long HAP nanorods with a unique orthorhombic shape were generated via a single-crystal-to-single-crystal transformation process from OCP nanorods, with preservation of the crystal morphology. In contrast, hexagonal HAP rods were obtained by splitting large, blade-like OCP particles in the absence of gelatin. Both bone and tooth enamel consist of apatite/biomolecule composites with several orders of hierarchical structures. The single-crystal-to-single-crystal transformation in nanocrystals allows transformation on the smallest scale, while leaving the structures in the higher hierarchy unperturbed. This may be an important principle in the construction of biomineral structures. Finally, we note that our bundles of HAP nanorods may be a good biomaterial for bone replacement in implantation. They possess simultaneously excellent mechanical strength and porosity, which would facilitate bone ingrowth in these materials.

4. Experimental

In a typical synthetic process, calcium nitrate ($Ca(NO_3)_2 \cdot 4H_2O$, 10 mmol), sodium dihydrogen phosphate dehydrate ($NaH_2PO_4 \cdot 2H_2O$,

10 mmol), and urea (20 mmol) were dissolved in an aqueous solution (500 mL) of gelatin (from lime-cured bovine skin, 225Bloom, 1 g L^{-1}, Sigma). Then, this solution was kept at 100 °C for 4 days. Finally, the product was filtered, washed with deionized water, and desiccated at 60 °C. XRD data were collected on a Scintag X1 diffractometer using CuKα radiation ($\lambda = 1.5418$ Å) in the 2θ range 3–60°. The SEM micrographs were taken on a JEOL-JSM-6700F field-emission scanning electron microscope. The TEM images and electron diffraction patterns were collected on a Hitachi H-7100 transmission electron microscope at 75 kV. All NMR experiments were carried out at a ^{31}P frequency of 121.5 MHz on a Bruker DSX300 NMR spectrometer equipped with a commercial 4 mm MAS NMR probe. All spectra were measured at a spinning frequency of 10 kHz. MAS frequency variation was limited to ±3 Hz using a commercial pneumatic control unit. The recycle delay was set to 60 s. ^{31}P chemical shifts were externally referenced to 85 % phosphoric acid.

Received: May 4, 2005
Final version: June 25, 2005
Published online: November 7, 2005

[1] a) J. L. Atwood, L. J. Barbour, A. Jerga, B. L. Schottel, *Science* **2002**, *298*, 1000. b) G. Kaupp, *Curr. Opin. Solid State Mater. Sci.* **2002**, *6*, 131. c) S. Takahashi, H. Miura, H. Kasai, S. Okada, H. Oikawa, H. Nakanishi, *J. Am. Chem. Soc.* **2002**, *124*, 10 944. d) D. H. Son, S. M. Hughes, Y. Yin, A. P. Alivisatos, *Science* **2004**, *306*, 1009.

[2] R. S. Bogadi, D. C. Levendis, N. J. Coville, *J. Am. Chem. Soc.* **2002**, *124*, 1104.

[3] a) D. B. Varshney, G. S. Papaefstathiou, L. R. MacGillivray, *Chem. Commun.* **2002**, 1964. b) V. Buchholz, V. Enkelmann, *Mol. Cryst. Liq. Cryst.* **2001**, *356*, 315.

[4] B. Rather, M. J. Zaworotko, *Chem. Commun.* **2003**, 830.

[5] M. Albrecht, M. Lutz, A. L. Spek, G. van Koten, *Nature* **2000**, *406*, 970.

[6] a) H. Cölfen, S. Mann, *Angew. Chem. Int. Ed.* **2003**, *42*, 2350. b) R. K. Tang, L. J. Wang, C. A. Orme, T. Bonstein, P. J. Bush, G. H. Nancollas, *Angew. Chem. Int. Ed.* **2004**, *43*, 2697.

[7] a) S. Mann, *Biomineralization Principles and Concepts in Bioinorganic Materials Chemistry*, Oxford University Press, New York **2001**. b) H. A. Lowenstam, S. Weiner, *Biomineralization*, Oxford University Press, New York **1989**.

[8] S. V. Dorozhkin, M. Epple, *Angew. Chem. Int. Ed.* **2002**, *41*, 3130.

[9] a) P. Bodier-Houllé, P. Steuer, J. Voegel, F. J. G. Cuisinier, *Acta Crystallogr. Sect. D* **1998**, *54*, 1377. b) M. Iijima, D. G. A. Nelson, Y. Pan, A. T. Kreinbrink, M. Adachi, T. Goto, Y. Moriwaki, *Calcif. Tissue Int.* **1996**, *59*, 377.

[10] a) S. Graham, P. W. Brown, *J. Cryst. Growth* **1996**, *165*, 106. b) M. Iijima, H. Kamemizu, N. Wakamatsu, T. Goto, Y. Doi, Y. Moriwaki, *J. Cryst. Growth* **1997**, *181*, 70. c) A. Bigi, E. Boanini, G. Cojazzi, G. Falini, S. Panzavolta, *Cryst. Growth Des.* **2001**, *1*, 239. d) Y. Liu, G. H. Nancollas, *J. Phys. Chem. B* **1997**, *101*, 3464.

[11] M. I. Kay, R. A. Young, A. S. Posner, *Nature* **1964**, *204*, 1050.

[12] a) A. C. Tas, *J. Am. Ceram. Soc.* **2001**, *84*, 295. b) K. Kandori, N. Horigami, A. Yasukawa, T. Ishikawa, *J. Am. Ceram. Soc.* **1997**, *80*, 1157. c) S. Ban, S. Maruno, *J. Biomed. Mater. Res.* **1998**, *42*, 387. d) R. Kniep, S. Busch, *Angew. Chem. Int. Ed. Engl.* **1996**, *35*, 2624. e) F. Peters, M. Epple, *J. Chem. Soc., Dalton Trans.* **2001**, 3585.

[13] a) W. E. Brown, *Nature* **1962**, *196*, 1048. b) W. E. Brown, J. R. Lehr, J. P. Smith, A. W. Frazier, *Nature* **1962**, *196*, 1050. c) W. E. Brown, L. W. Schroeder, B. Dickens, *J. Crystallogr. Spectrosc. Res.* **1988**, *18*, 235.

[14] M. Iijima, H. Kamenmizu, N. Wakamatsu, T. Goto, Y. Doi, Y. Moriwaki, *J. Cryst. Growth* **1997**, *181*, 70.

[15] J. Zhan, H. P. Lin, C. Y. Mou, *Adv. Mater.* **2003**, *15*, 621.

[16] A. Bigi, B. Elisa, S. Panzavolta, N. Roveri, *Biomacromolecules* **2000**, *1*, 752.

[17] S. Eiden-Assmann, M. Viertelhaus, A. Heiss, K. A. Hoetzer, J. Felsche, *J. Inorg. Biochem.* **2002**, *91*, 481.

[18] S. Busch, U. Schwarz, R. Kniep, *Adv. Funct. Mater.* **2003**, *13*, 189.

[19] a) A. Bigi, E. Boanini, B. Bracci, G. Falini, K. Rubini, *J. Inorg. Biochem.* **2003**, *95*, 291. b) A. Bigi, E. Boanini, M. Gazzano, K. Rubini, P. Torricelli, *Biomed. Mater. Eng.* **2004**, *14*, 573. c) A. Bigi, B. Bracci, S. Panzavolta, M. Iliescu, M. Plouet-Richard, J. Werckmann, D. Cam, *Cryst. Growth Des.* **2004**, *4*, 141.

[20] M. Iijima, Y. Moriwaki, T. Takagi, J. Moradian-Oldak, *J. Cryst. Growth* **2001**, *222*, 615.

[21] M. Iijima, J. Moradian-Oldak, *J. Mater. Chem.* **2004**, *14*, 2189.

[22] D. B. Williams, C. B. Carter, *Transmission Electron Microscopy*, Plenum, New York **1996**, p. 247.

[23] Y. H. Tseng, J. Zhan, K. S. Lin, C. Y. Mou, J. C. Chan, *Solid State Nucl. Magn. Reson.* **2004**, *26*, 99.

[24] A. G. Ward, A. Courts, *The Science and Technology of Gelatin*, Academic, New York **1977**.

[25] D. Hanein, B. Geiger, L. Addadi, *Langmuir* **1993**, *9*, 1058.

[26] a) M. E. Fernandez, C. Zorrilla-Cangas, R. Garcia-Garcia, J. A. Ascencioc, J. Reyes-Gasgab, *Acta Cryst. B* **2003**, *B59*, 175. b) G. Falini, M. Gazzano, A. Ripamonti, *J. Mater. Chem.* **2000**, *10*, 535.

[27] a) N. M. Hancox, *Biology of Bone*, Cambridge University Press, Cambridge, UK, **1972**. b) R. Lakes, *Nature* **1993**, *361*, 511.

